JOURNAL OF THE KOREAN ASTRONOMICAL SOCIETY
**35**: 175 ~ 185, 2002

# LY$\alpha$ LINE FORMATION IN HUBBLE-TYPE SPHERICAL OUTFLOWS IN STARBURST GALAXIES

SANG-HYEON AHN[1] AND HEE-WON LEE[2]
[1]Korea Institute for Advanced Study
[2]Department of Astronomy, Sejong University, Seoul, Korea
*E-mail: sha@kias.re.kr*
*(Received Nov. 10, 2002; Accepted Nov. 21, 2002)*

## ABSTRACT

Almost half of primeval galaxies show P-Cygni type profiles in the Ly$\alpha$ emission line. The main underlying mechanism for the profile formation in these systems is thought to be the frequency redistribution of the line photons in expanding scattering media surrounding the emission source. A Monte Carlo code is developed to investigate the Ly$\alpha$ line transfer in an optically thick and moving medium with a careful consideration of the scattering in the damping wings. Typical column densities and expansion velocities of neutral hydrogen investigated in this study are $N_{HI} \sim 10^{17-20}$ cm$^{-2}$ and $\Delta V \sim 100$ km s$^{-1}$. We investigate the dependence of the emergent profiles on the kinematics and on the column density. Our numerical results are applied to show that the damped Ly$\alpha$ absorbers may possess an expanding H I supershell with bulk flow of $\sim 200$ km s$^{-1}$ and H I column density $N_{HI} \sim 10^{19}$ cm$^{-2}$. We briefly discuss the observational implications.

*Key words :* early Universe — galaxies: starburst — radiative transfer — line: formation — line: profiles

## I. INTRODUCTION

High-redshift galaxies are usually observed by recent spectroscopic observations in debt of big telescopes and space telescopes. The high-redshift galaxies show themselves up on the spectra of high-redshift quasars by features blueward of the broad Ly$\alpha$ emission line. The former are usually called the Lyman break galaxies, the Ly$\alpha$ emitting galaxies, and the quasars' companion galaxies. Also the latter include the damped Ly$\alpha$ absorbers (DLAs), the Lyman limit systems(LLSs), and the metallic line systems (MLAs).

The first rest-frame UV spectra of DLAs is that of DLA 2233+131 (Djorgovski et al. 1996), which has a Ly$\alpha$ emission line. It is an interesting fact that the emission line shows the asymmetry in the sense that the blue shoulder is stiffer than the red part. Also the width of the emission is as large as 300 km s$^{-1}$, which was attributed to the galactic rotation. In the meanwhile, Prochaska & Wolfe (1997) analyzed the absorption line profiles of the 17 DLAs obtained with the HIRES eschelle spectrograph on the Keck telescope and concluded that the kinematics of the DLAs supports the hypothesis that they are rapidly rotating "cold" disks (see also Haehnelt, Steinmetz, & Rauch 1998). However, it turns out that the broad emission is due to the outflowing material surrounding the Ly$\alpha$ source (Kunth et al. 1998; Lee & Ahn 1998; Ahn, Lee, & Lee 2003).

After the discovery of DLA 2233+131, Djorgovski et al. (1997) found a number of new DLA candidates (see also Djorgovski 1998). In addition to these DLA candidates, there are many primeval galaxies which show Ly$\alpha$ emission in their spectra.

Currently, there are a few observational programs to discover and study primeval galaxies at $z > 3$. The first one is to search for the DLA candidates by deep imaging and spectroscopic observations(Möller & Warren 1993, Warren & Möller 1996; Djorgovski et al. 1996). In a similar way, primeval galaxies have been found as quasar companions (Hu, McMahon, & Egami 1996; Petitjean et al. 1996).

Another method is narrow-band Ly$\alpha$ imaging and subsequent spectroscopic confirmation. Adopting this method, Hu et al. (1998) found a primeval star-forming galaxy with a very high redshift being at $z = 5.64$(see also Cowie & Hu 1998).

The third one is the Lyman-break method for star-forming galaxies in $3 < z < 3.5$ (Steidel et al. 1996a, 1996b, 1998; Pettini et al. 2001). The Ly$\alpha$ emission features of these galaxies exhibit P-Cygni type profiles. According to a deeper and higher resolution imaging observations (Giavalisco et al. 1996), these objects appear to be compact spheroidal cores often surrounded by low surface brightness nebulosities. Assuming the standard cosmology of $\Omega_0 = 1$ and $H_0 = 50$ km s$^{-1}$ Mpc$^{-1}$, a typical size of the cores is a few kpc. The authors suggested that these are the bulges of the primeval galaxies that are precursors of nearby normal galaxies. Lowenthal et al. (1997) applied the similar color criteria successfully to find primeval galaxies having P-Cygni type profiles in the

*Corresponding Author*: S.-H. Ahn

Hubble Deep Field at $z \simeq 3$.

Another program is provided by gravitational lenses (Franx et al. 1997, Trager et al. 1997, Frye & Broadhurst 1998, Dey et al. 1998). This method now becomes a powerful tool, because the magnification of gravitational lens enables one to detect more distant objects than other methods permit.

Among these the Lyman Break method is the most successful, and now give us about thousand profiles (Adelberger et al. 2002). It is particularly interesting to note that nearly half of these objects show Ly$\alpha$ emission line feature, each of which is often accompanied by a P-Cygni type absorption trough. We note that P-Cygni type Ly$\alpha$ profiles are prevailing in both nearby starbursting galaxies and remote primeval galaxies (Marlowe et al. 1995; Martin 1998; Heckman, Armus, & Miley 1990; Kunth et al. 1998; Steidel et al. 1999; Pettini et al. 2001). It is a general consensus that the Ly$\alpha$ emission features are originated from star-forming regions. This statement has been supported by the fact that the galaxy discovered by Frye & Broadhurst (1998) shows several bright knots of star-forming regions which show P-Cygni type Ly$\alpha$ emission, as well as the considerable portion of arcs which do not show Ly$\alpha$ emission but are composed of stellar light (Bunker et al. 1997). It is also notable that galactic superwinds are often found in nearby starbursting galaxies and that the P-Cygni type Ly$\alpha$ lines are believed to be associated with the outflows of kpc scale. Thus, we propose that the P-Cygni profile of the Ly$\alpha$ emission line can be interpreted to be formed from an expanding medium that envelops the emission source. There are mainly two types of outflows in starburst galaxies. One is the galactic supershell, and the other is the galactic winds. We have already investigated the galactic supershell (Ahn et al. 2003), and so we study in this paper the Ly$\alpha$ radiative transfer in a galactic wind surrounding the super star cluster supposedly located near the center of a starburst galaxy.

This paper is composed as follows. We describe a superwind model and the computation method in section II, as well as Appendix. In section III the main results are presented. In the last section is given a brief discussion in relation to the implications for the identity of primeval galaxies. We give a summary and conclude in the final section.

## II. GALACTIC SUPERWIND MODEL AND MONTE CARLO SIMULATIONS

### (a) Galactic Superwind Model

The ambient media surrounding nearby star-forming regions often show outflows that are driven by starburst activity. According to some theories (e.g. Lehnert & Heckman 1996, Suchkov et al. 1994), the starburst driven wind is initiated by multiple supernovae explosions leaving hot cavities. The initial stage is highly adiabatic because there is little time for radiative cooling. The injected energy is consumed to form a bubble that expands and sweeps out the ambient medium. The radiative cooling becomes important and typically a thin shell forms. This shell is known to be subject to the Rayleigh-Taylor instability and subsequently breaks up.

Then the outer medium can be swept up by the leaked hot gas and newly forms another shock, which ionizes the outer region. After all, the enveloping ionized media expand into the intergalactic space because of the pressure enhancement. Observationally, the outflows found in M82 (McKeith et al. 1995) and Mrk 1259 (Ohyama, Taniguchi, & Terlevich 1997) are good examples, and these outflows are often called "galactic superwinds" (Heckman, Armus, & Miley 1990). The interiors of these media are isobaric within a factor of two. Hence, we assume that the galactic superwinds are a sort of partially ionized bubble that expands like a bubble.

The first example we consider is the H I supershells and the worms/chimneys in our Galaxy (Heiles 1979, 1984: Koo, Heiles, & Reach 1991, 1992; Reach, Heiles, & Koo 1993) and nearby galaxies. An especially large H I supershell is known to be found in the nearby normal spiral galaxy M101 (Kamphuis et al. 1991). In M101, the measured line-of-sight expanding velocity component of the supershell amounts to $\sim 50$ km s$^{-1}$. The H I column density of the supershell is estimated to be $N_{HI} \simeq 2 \times 10^{20}$ cm$^{-2}$. The supershell must be bipolar in shape rather than spherical. Two-dimensional calculations of the evolution of the supershell generated by strong mechanical energy deposited by young star clusters in dwarf galaxies was studied by Silich & Tenorio-Tagle (1998). The evolution of superbubbles and the schematic description on the Ly$\alpha$ emergent profiles can be seen in Tenorio-Tagle et al. (1999). The possibility of the formation of P-Cygni type Ly$\alpha$ line in the supershell is investigated in Ahn, Lee and Lee (2003) and Ahn (2003).

In this study, the kinematics and distribution of the scatterers are strongly constrained by the existence of the observed P-Cygni profile. That is, P-Cygni profiles are usually formed in a system consisting of a compact radiation source surrounded by a scattering component with a non-negative velocity gradient. In this paper we choose to investigate the positive velocity gradient case leaving the zero velocity gradient case as a future work, which corresponds to the shell case.

The density profile and the velocity profile of the winds should be functions of the radius ($r$). When the media is thin and the velocity gradient is much larger than the thermal speed, we can adopt the Sobolev approximation. In this approximation we consider only the core scattering. However, it is quite different if the Ly$\alpha$ opacity at the wing becomes important. We cannot neglect the wing scattering, and the Sobolev approximation breaks down. Hence, we have only to assume that the outflow of the scattering medium is

characterized by a Hubble-type velocity field with a uniform density. The medium is also assumed to be density bounded, that is, it is dominated by ionized hyrogen with a small uniform fraction of neutral component. Usually we expect that the density profile has a form of a decreasing function of radius, and our assumptions do violate mass flux conservation. Yet, we consider the solution can give us some first-order insight to the problem.

The homogeneity of the scattering media is also assumed in order to make the probelm simple. The outflowing media is surely apt to be fragmented into inhomogeneous media, which will affect the formation of emegent Ly$\alpha$ profiles. However, it is practically very hard to solve such a problem. Hence, we will assume that the outflowing media have no irregularity in density profile.

The main emission region is effectively limited to a compact central region, because the emission measure is proportional to $n_e^2$. Here $n_e$ is the electron density. Therefore, in the Monte Carlo computation adopted in this work, we will assume that the moving medium is a purely scattering one and that there exists a point-like emission source located at the center. Since the main concern in the current work is to understand the characteristic properties of the physical environments around the star forming region, the assumptions render the problem simpler and serve our purposes despite the fact that it is a toy model.

In order to understand the physical configuration of the central region where most of the observed Ly$\alpha$ photons are generated, we check a number of physical quantities. Djorgovski et al. (1996) reported that assuming a standard Friedman cosmology with $H_0 = 75$ km s$^{-1}$Mpc$^{-1}$ and $\Omega_0 = 0.2$, the angular diameter distance to DLA 2233+131 is $1.96 \times 10^{28}$ cm, the luminosity distance $r_L = 8.14 \times 10^{28}$ cm, and the observed Ly$\alpha$ line flux $F_{1216}$ is

$$F_{1216} = (6.4 \pm 1.2) \times 10^{-17} \text{ erg cm}^{-2} \text{ s}^{-1}. \quad (1)$$

We assume in this paper that the H II region is a sphere of radius $R$ for reasons of simplicity. Then the observed Ly$\alpha$ line flux is approximately given by

$$F_{1216} \simeq \frac{(h\nu_0)\alpha_B(n_e n_p)}{4\pi r_L^2} V_{HII}, \quad (2)$$

where $n_e$ is the electron density, $n_p$ is the proton density, $V_{HII}$ is the volume of the H II region, and the case B recombination coefficient $\alpha_B = 2.59 \times 10^{-13}$ cm$^3$ s$^{-1}$ for $T = 10^4$ K (Osterbrock 1989).

From Eq.(1) and Eq.(2), we obtain the electron density $n_e$,

$$n_e \simeq 4 \left(\frac{1 \text{ kpc}}{R}\right)^3 \text{ cm}^{-3}. \quad (3)$$

If we extrapolate the correlation between the velocity dispersion and the radius of giant H II regions (Terlevich & Melnick 1981) and use the velocity dispersion $\sim 300$ km s$^{-1}$ of the H II region in DLA 2233+131, then its size is estimated to be $R \sim 1$ kpc. Assuming that the emission region is fully ionized, we obtain the total mass of the central H II region

$$M_{HII} \simeq 10^8 M_\odot. \quad (4)$$

Because one O5 star typically generates UV photons at a rate of $5 \times 10^{49}$ photons s$^{-1}$ (Spitzer 1978), it follows that the number of O5 stars needed to account for the Ly$\alpha$ flux in DLA 2233+131 is $\sim 10^3$ under the assumption that the H II region is ionized purely by these O5 stars. According to Kennicutt et al. (1989), the first-ranked H II regions found in nearby spirals and irregulars require the total mass of the ionizing stars ($> 10\ M_\odot$) ranging $10^2 - 10^6\ M_\odot$. This is consistent with the assumption that the Ly$\alpha$ emission line from DLA 2233+131 is originated from these first-ranked H II regions.

Furthermore, we assume the neutral column density of the outer expanding scattering medium to be $N_{HI} \gtrsim 10^{17}$ cm$^{-2}$, which is prevailing in the nearby starbursts (e.g. Conti, Leitherer, & Vacca 1996). With this estimate of the HI content, the medium is nearly matter-bounded, and the required ionization fraction $n_{HI}/n_{HII} \gtrsim 10^{-4}$. This estimate is also supported by the facts that the Ly$\alpha$ profile shows the black absorption trough and that the spectrum of the DLA does not shows any Ly$\beta$ emission.

It is very interesting that the physical parameters derived above are similar to the Lyman break galaxies (Ahn, Lee & Lee 2002), and also to the host galaxies of gamma ray bursts (Ahn 2000). For more detailed argument for the astrophysical parameters can be consulted in Ahn (2003). Also the astrophysical meaning of these facts related with the identity of the populations of primeval galaxies are going to be dealt in the final discussion section.

### (b) Computation Method

In this subsection we give a brief description of the Monte Carlo code, which computes the profile of the emergent Ly$\alpha$ photons scattered in an optically thick and expanding medium. The relevant description of the method as well as some related topics can be found in our other papers (Ahn et al. 2000, 2001, 2002). The Ly$\alpha$ profiles in the primeval galaxies are observed to show black troughs, which indicates that the enveloping neutral media have high optical depths. Another important point is provided by the non-detection of Ly$\beta$ emission, which is easily destroyed in an optically thick medium via non-coherent scatterings (or resonant Raman scatterings) that produce H$\alpha$ emission.

So far, many investigations about the formation processes of the P-Cygni profile have been concentrated on the outflowing systems possessing rather moderate optical depths. In this case, the Sobolev approximation is regarded as a powerful method to understand the behavior of resonantly scattered photons in an expanding

medium with a bulk flow speed much larger than the thermal speed (e.g. Sobolev 1960, Mihalas 1978). In the cases of optically thick media, scatterings in the damping wings are not negligible any more and the validity of the Sobolev approximation becomes questionable. Therefore, in this work, we adopt a Monte Carlo approach to deal with the radiative transfer of Ly$\alpha$ photons in an optically thick and expanding medium.

As mentioned in the previous section, we adopt a simple kinematic model, in which the compact radiation source is surrounded by a spherical scattering medium with radius $r_{max}$. The velocity field of the scattering medium is assumed to be given by a Hubble-type flow, i.e.,

$$\mathbf{v} = H_v \mathbf{r}, \tag{5}$$

where $H_v$ is the bulk flow velocity gradient, $\mathbf{v}$ is the bulk velocity, and $\mathbf{r}$ is the distance from the center of the velocity field. In this type of velocity field, the distance is more conveniently measured by the parameter $s$ defined by

$$s \equiv H_v r / v_{th}, \tag{6}$$

where $v_{th}$ is the thermal velocity.

If we introduce the Doppler width $\Delta\nu_D$ defined by

$$\Delta\nu_D \equiv \nu_0 \frac{v_{th}}{c}, \tag{7}$$

then the frequency of a line photon is also conveniently described by the normalized frequency shift $x$ defined by

$$x \equiv (\nu - \nu_0)/\Delta\nu_D. \tag{8}$$

In order to determine the subsequent scattering position in the Monte Carlo calculation, the scattering optical depth $\tau_{12}(x)$ corresponding to the distance between the positions $\mathbf{r_1}$ and $\mathbf{r_2}$ is computed to be

$$\begin{aligned} \tau_{12}(s) &= \tau_0 \int_{-\infty}^{\infty} du\, e^{-u^2} \left[ \tan^{-1}\left(\frac{u+x}{a}\right) \right. \\ &- \left. \tan^{-1}\left(\frac{u+x-s}{a}\right) \right]. \end{aligned} \tag{9}$$

Here, $\tau_0$ is the Sobolev-type optical depth defined by

$$\tau_0 = \frac{\pi e^2}{mc} f_{osc} \frac{n_o}{\pi^{3/2}} \frac{\lambda_0}{H_v} \tag{10}$$

(Sobolev 1960), and $a$ is the damping coefficient normalized by $\Delta\nu_D$, i.e.,

$$a = \Gamma / 4\pi\Delta\nu_D, \tag{11}$$

where $\Gamma$ is the damping constant.

The inverse transformation of Eq.(9) is performed numerically to find the normalized path length $s$ corresponding to a given scattering optical depth $\tau_{12}$. The conversion of the H I column density and the Sobolev type optical depth $\tau_0$ is then given by

$$\left(\frac{\tau_0}{10^4}\right) = \left(\frac{N_{HI}}{4.1 \times 10^{18}\ \mathrm{cm^{-2}}}\right) \left(\frac{H_v \cdot r_{max}}{100\ \mathrm{km\ s^{-1}}}\right)^{-1} \left(\frac{f_{osc}}{0.4162}\right) \tag{12}$$

where $N_{HI} = n_0 r_{max}$. A more detailed description of the Monte Carlo computational procedure is given in Appendix. The new features in the Monte Carlo code include an exact treatment of the partial frequency redistribution by computing the accurate probability according to which we determine the scattering type. This point is very important because the escape of a line photon is usually made when the scattering occurs in the damping wing regime. Moreover, the scattering phase function for a damping wing scattering is different from that for a resonant scattering, and this point is of particular importance when the polarization is to be measured (e.g. Lee & Ahn 1998). However, in this work, we concentrate on the line formation process and the main result is quite insensitive to the choice of the exact phase functions.

## III. RESULTS

### (a) Emergent Profiles and Line Formation Mechanism

In Fig. 1 we show the emergent Ly$\alpha$ profile from a thick expanding medium. The horizontal axis represents $\Delta\lambda/\Delta\lambda_D = -x$, and the vertical axis stands for the flux. Note that the wavelength deviation is the negative of the frequency deviation and that $\Delta\lambda_D$ is the Doppler width in wavelength. The emission source lying in the center of the scattering medium is assumed to be governed by a Gaussian profile with the width $\sigma_x = 5$. We choose $v_{th} = 10$ km s$^{-1}$, $s_{max} = 10$, which corresponds to $\Delta V_{bulk} = 100$ km s$^{-1}$. We also choose $\tau_0 = 10^4$ that leads to $N_{HI} = 4.1 \times 10^{18}$ cm$^{-2}$ given the above choice of $s_{max}$.

The main features in the emergent profile in Fig. 1 include a primary peak in the red part and a much weaker secondary peak in the blue part. The line formation is affected by the diffusion both in frequency space and in real space due to the presence of velocity field exceeding the thermal speed in a thick medium.

When a static medium has a moderate line center optical depth $\tau_c < 10^5$, the radiative transfer is dominated by the diffusion in frequency space, and the spatial diffusion plays a minor role. Hence each photon is scattered many times in the vicinity of its source and gets a sufficient frequency shift just before it escapes, which Adams (1972) described as "a single longest flight." The frequency shift occurs when the Ly$\alpha$ photon scatters with a rapidly moving hydrogen atom in the tail of the Boltzmann distribution. For a thicker medium with $\tau_c \gtrsim 10^5$, the damping wing scattering becomes important, and the photons emerge via the spatial diffusion. This process was called "a

single longest excursion" by Adams (1972). He investigated these processes using a Monte Carlo method and showed that the mean scattering number $\langle N \rangle$ before escape is given by

$$\langle N \rangle \approx \begin{cases} \tau_c \sqrt{\pi \ln \tau_c} & \text{for } \tau_c < 10^5 \\ 1.5\pi^{1/2}\tau_c & \text{for } \tau_c > 10^5. \end{cases} \quad (13)$$

In the Sobolev theory for a resonance shell having a width of velocity difference of order $v_{th}$ in an expanding medium, the effective optical depth is the Sobolev scattering optical depth $\tau_0$ that coincides with the total scattering optical depth in the limit $\Delta V \to 0$. However, this hypothesis works only when $\tau_0 \lesssim 10^3$, in which case a frequency diffusion into the red wing leads to a direct escape from the scattering medium without further scattering in the damping wing.

When $\tau_0 \geq 10^4$, the damping wing scattering optical depth is not negligible and the line photon can be captured with significant probability despite the frequency diffusion into the red wing. The subsequent scatterings tend to reduce the frequency deviation of the line photon as the restoring force in the frequency space operates (see Adams 1972). Therefore, the line photon is again resonantly scattered after several wing scatterings accompanied by severe spatial movements. In this case, the total scattering number is dominantly affected by the total column density of the scattering medium, which is proportional to the product of $\tau_0$ and $s_{max}$ according to Eq.(12).

Therefore, when $\tau_0 = 10^4$ and $s_{max} = 10$, the scattering number before escape is expected to be of order $10^5$ by regarding the resonance shell as a static medium with a line center optical depth $\tau_c \sim \tau_0$ (Adams 1972). We have checked that the scattering number increases almost linearly with $\tau_0 s_{max}$.

In Fig. 2 is shown a typical scattering behavior of a photon with $x_{init} \sim 0$. The horizontal axis represents the scattering number. In the bottom panel is shown the frequency variation of the photon. In the middle panel, we show the radial distance of the photon from the center of the sphere with radius $s = 10$. The scattering type is shown in the top panel in which we denote a wing scattering by 0 and a resonance scattering by 1.

Near the 360th scattering, the frequency of the photon deviates much from the center frequency, and several scatterings in the damping wing follow. During this process, the photon propagates a large distance in real space and becomes resonant again by the effect of the restoring force (in frequency space) stated by Adams (1972). When the photon escapes from the medium, it experiences several wing scatterings, and the frequency of the photon falls on the red part.

In Fig. 3 we show a typical scattering behavior of a blue photon with the input frequency $x_{init} \sim 5$. Initially it experiences several damping wing scatterings and propagates easily with a large free path until it hits the resonance zone. Once it enters the resonance

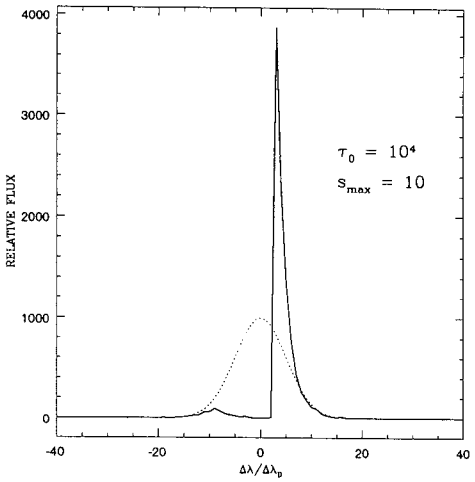


**Fig. 1.**— The emergent Ly$\alpha$ profile from a thick expanding medium. The horizontal axis represents $\Delta\lambda/\Delta\lambda_D$ and the vertical axis for the relative flux. The emission source is assumed to be given by a Gaussian profile $\propto e^{-(x/2\sigma_x)^2}$, where the width $\sigma_x$ is set to be 5. We choose $s_{max} = 10$ and $\tau_0 = 10^4$. The emergent profile is represented by the solid line and the dotted line shows the initial Gaussian profile.

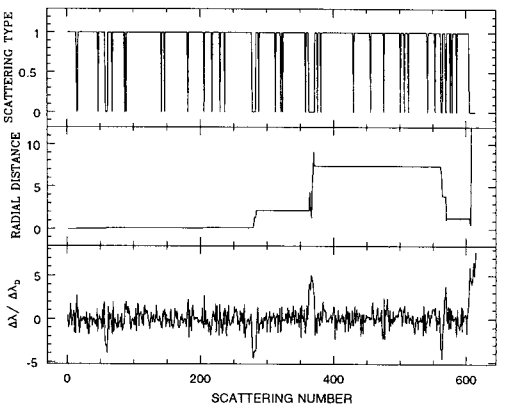


**Fig. 2.**— Typical scattering behaviors of Ly$\alpha$ line photons. The initial frequency of a photon at the time of creation is $x_{init} = 0$. The horizontal axis stands for the scattering number. In the bottom frequency deviation is shown, and in the top panel the scattering type is given, where 0 stands for a wing scattering and 1 for a resonant scattering. In the middle panel the radial distance of the photon is shown.

regime, the photon experiences the similar processes to those of the red photons described above.

On the other hand, majority of the extremely blue and the extremely red photons escape the medium with at most several damping wing scatterings.

### (b) Dependence on Kinematics and Column Density

In Fig. 4, we show the emergent profiles for the values of $s_{max} = 1$, 2, 5, 10, and 20, and for a fixed value of $\tau_0 = 10^4$. The profile variation is dominated by the coupled effects of the kinematics and column density of the medium.

When $s_{max} \to 0$, the profile becomes symmetric, as is naturally expected in the static case. As $s_{max}$ becomes large for a given optical depth, the flux of the red part becomes stronger than the blue counterpart because the kinematics becomes important. This implies that the flux ratio of the red part to that of the blue part may be a useful parameter to determine the kinematics and column density of the medium.

In Fig. 5, we show the profiles for various values of $s_{max}$ keeping $\tau_0 = 10^5$. The profiles shown in Fig. 5 differ in detail from those shown in Fig. 4. In particular, the peak positions of the red part recedes as $s_{max}$ increases. However, the end points of the absorption trough remain unchanged, which are located at $\Delta\lambda/\Delta\lambda_D \sim \pm 2$. Therefore, the slope of the profile between the red peak and the starting point of the absorption trough $\Delta\lambda/\Delta\lambda_D \sim 2$ decreases monotonically as $s_{max}$ increases when $\tau_0 = 10^5$.

This behavior is obtained because the effective optical depth of the medium gets larger as the $s_{max}$ grows larger. However, the line center optical depth also affects the slope of the red edge in the primary peak in a coupled manner. This also implies that the slope of the profile at the red edge of the primary peak can be useful to extract the physical quantities such as the $s_{max}$ and $\tau_0$ from the observed profiles.

In Fig. 6 are shown the emergent profiles for moderate column densities, $\tau_0 = 10^3$, $10^4$, $10^5$, and $10^6$ for a fixed $s_{max} = 10$. The primary red peak recedes to the red, as the column density increase. The slope of the central edge of the primary red peak exhibits variations similar to those of the previous cases shown in Fig. 6.

When $\tau_0$ is extremely large, the red and the blue peaks appear to be a big wide bump, and their fluxes becomes rather symmetric. This means that as the line center optical depth becomes extremely large the kinematics plays a minor role. In other words, the mean propagation length of a photon in the extremely thick medium is so small that the kinematic effects by the Hubble-type velocity becomes negligible.

## IV. SUMMARY AND CONCLUSION

We have studied the line transfer in an optically thick and moving medium including the damping wing

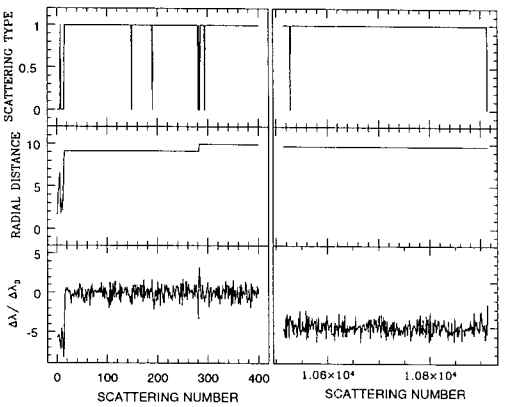


**Fig. 3.**— A typical scattering behavior for a Ly$\alpha$ line photon with $x_{init} = 5$. All other quantities are the same as in Fig. 2. Note that the average frequency in the lower right panel is $x = 0$, and that the ordinate label on the left panel is not applied to the right panel.

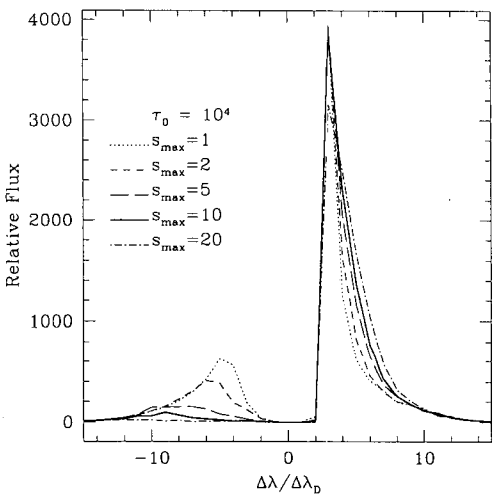


**Fig. 4.**— The emergent Ly$\alpha$ profiles for various bulk velocity scales $s_{max}$ of the scattering medium. We fix $\tau_0 = 10^4$ and the initial Gaussian profile having a width of $\sigma_x = 5$ is used. The dotted line is for the case of $s_{max} = 1$, the dashed line for $s_{max} = 2$, the long dashed line for $s_{max} = 5$, the solid line for $s_{max} = 10$, and the dot-dashed line for $s_{max} = 20$.

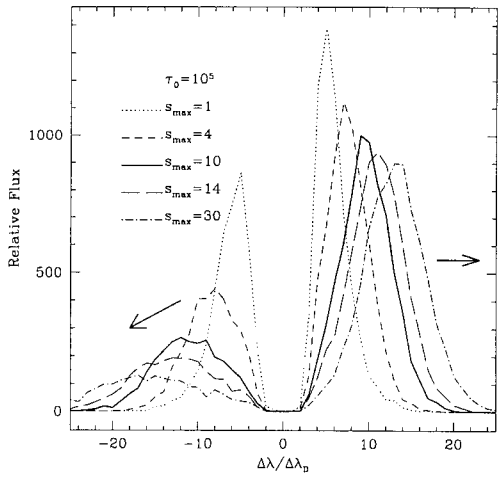


**Fig. 5.**— The emergent Ly$\alpha$ profiles for various bulk velocity scales $s_{max}$ with fixed $\tau_0 = 10^5$. The dotted line is for $s_{max} = 1$, the dashed line for $s_{max} = 4$, the thick solid line for the case of $s_{max} = 10$, the long dashed line for $s_{max} = 14$, and the dot-dashed line for $s_{max} = 30$.

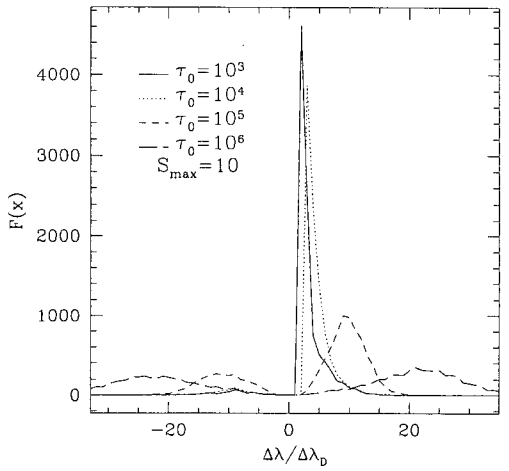


**Fig. 6.**— The emergent Ly$\alpha$ profiles for Sobolev type optical depths $\tau_0$ of the scattering medium not exceeding $10^4$. We use a fixed $s_{max} = 10$ and the initial Gaussian profile having a width of $\sigma_x = 5$. The solid line represents the profile for $\tau_0 = 10^3$, the dotted line for $\tau_0 = 10^4$, the dashed line for $\tau_0 = 10^5$, and the dot-dashed line for $\tau_0 = 10^4$.

scattering using a Monte Carlo method. The emergent profiles are characterized by the asymmetric double peaks with a primary peak in the red part, a secondary peak in the blue part, and an absorption trough in the blue. The underlying mechanisms for the transfer and the dependence of the emergent profiles on the H I column density and on the kinematics were investigated. The primary red peak recedes to the red as $N_{HI}$ increases, and for thicker media with $\tau_0 \geq 10^6$ the Ly$\alpha$ line profile is characterized by two separated broad humps. It is also found that as $s_{max}$ gets smaller, symmetric double peak profiles are obtained, which is regarded as the static limit where bulk motion becomes negligible. It is proposed that the ratio of the flux of the red part to that of the blue part and the slope of the central edge of the primary red peak can be particularly useful to extract information about the kinematics and the H I column density of the scattering medium.

We can apply this method to explain the P-Cygni type Ly$\alpha$ emission in the spectra of primeval galaxies assuming that it is caused by expanding media with high H I column densities. Assuming nearly complete ionization, we deduced that the H II region in DLAs is characterized by the electron density $n_e \simeq 1$ cm$^{-3}$, the size $R \simeq 1$ kpc, and $M_{HII} \simeq 10^8 M_\odot$. To account for the Ly$\alpha$ line flux of a typical DLA about $10^3$ massive young stars are needed, which is consistent with the hypothesis that DLA is one of the first-ranked H II regions found in nearby spirals and irregulars. The slope at central edge of the primary peak gives a strong constraint on $\tau_0$ and we find that $\tau_0 \simeq 10^5$. Noting that the expanding bulk velocity $\Delta V_{bulk} \approx 200$ km s$^{-1}$, the column density responsible for the P-Cygni type feature is deduced to be $N_{HI} \simeq 10^{20}$ cm$^{-2}$.

A recent spectroscopic observations reveal that DLAs appear to reside in different environments than LBGs (Adelberger 2002). Also other work have reached the similar conclusion based upon different background (Fynbo, Möller, & Warren 1999; Mo, Mao & White 1999; Haehnelt, Haehnelt, Steinmetz, & Rauch 2000). However, the physical characteristics of starburst activities for DLAs and LBGs does not look different from each other. To be specific, the star formation rate from the Ly$\alpha$ luminosity from these two kinds of objects are not so different. However, this impression should be quantitatively proved, and the theoretical research on the dust extinction and the kinematic effects on the survival of Ly$\alpha$ should be done in the future.

## ACKNOWLEDGEMENTS

We are grateful to Prof. Bon-Chul Koo for careful and critical discussions on the galactic superwind model. SHA thanks Dr. Crystal Martin for useful discussion on the pressure within galactic superbubbles. Prof. Roger Blandford, Prof. Art Wolfe, Dr. Kee-Tae Kim, Prof. Hyung Mok Lee provided kind and helpful discussions for this work. We also thank the anonymous referee for useful corrections and sugges-

tions. HWL gratefuly acknowledges support from the Astrophysical Research Center for the Structure and Evolution of the Cosmos (ARCSEC) funded by Korea Science & Engineering Foundation.

## REFERENCES

Adams, T. 1972, The Escape of Resonance-Line Radiation from Extremely Opaque Media, ApJ, 174, 439

Adelberger, C., Steidel, C. C., Shapley, A. E., & Pettini, M., 2002, Galaxies and Intergalactic Matter at Redshift z 3: Overview, To Appear in ApJ (astro-ph/0210314)

Ahn, S. -H. 2000, Environment of the Gamma-Ray Burst GRB 971214: A Giant H II Region Surrounded by a Galactic Supershell, ApJ, 530, L9

Ahn, S. -H., Lee, H. -W., & Lee, H. M. 2000, Ly Alpha Transfer in a Thick, Dusty, and Static Medium, JKAS, 33, 29

Ahn, S. -H., Lee, H. -W., & Lee, H. M. 2001, Ly$\alpha$ Line Formation in Starbursting Galaxies. I. Moderately Thick, Dustless, and Static H I Media, ApJ, 554, 604

Ahn, S. -H., Lee, H. -W., & Lee, H. M. 2002, Ly$\alpha$ Line Formation in Starbursting Galaxies. II. Extremely Thick, Dustless, and Static H I Media, ApJ, 567, 922

Ahn, S. -H. 2003, submitted to MNRAS

Ahn, S. -H., Lee, H. -W., & Lee, H. M. 2003, P-Cygni Type Ly$\alpha$ from Starburst Galaxies, MNRAS, submitted (astro-ph/0204004)

Bunker, A. J., Moustakas, L. A., Davis, M., Frye, B. L., Broadhurst, T. J., & Spinrad, H. 1997, "The Young Universe: Galaxy Formation and Evolution at Intermediate and High Redshift" (Rome Observatory, 29 Sept - 3 Oct 1997) eds. S. D'Odorico, A. Fontana and E. Giallongo, A.S.P. Conf. Ser

Conti, P. S., Leitherer, C., & Vacca, W. D. 1996, Hubble Space Telescope Ultraviolet Spectroscopy of NGC 1741: A Nearby Template for Distant Energetic Starbursts, ApJ, 461, L87

Cowie, L., & Hu, E. M. 1998, High-z Ly alpha Emitters. I. A Blank-Field Search for Objects near Redshift Z = 3.4 in and around the Hubble Deep Field and the Hawaii Deep Field SSA 22, AJ, 115, 1319

Dey, A., Spinrad, H., Stern, D., Graham, J. R. & Chaffee, F. H. 1998, A Galaxy at z=5.34, ApJ, 498, L93

Djorgovski, S. G., Pahre, M. A., Bechtold, J., & Elston R., 1996, Identification of a galaxy responsible for a high-redshift Lyman-alpha absorption system, Nature, 382, 234

Djorgovski, S. G. 1997, Structure and Evolution of the IGM from QSO Absorption Line Systems, IAP Colloquium, eds. P. Petitjean and S. Charlot, in press

Djorgovski, S. G. 1998, astro-ph/9805159, "*Fundamental Parameters in Cosmology, XXXIII Recontres de Moriond*", eds. Y. Giraud-Héraud et al., Giff sur Yvette

Franx, M., Illingworth, G. D., Kelson, D., van Dokkum, P., & Tran, K. 1997, A Pair of Lensed Galaxies at z=4.92 in the Field of CL 1358+62, ApJ, 486, 75

Frye, B., & Broadhurst, T. 1998, Discovery of Red Selected Arcs at Z = 4.04 behind Abell 2390, ApJ, 499, L115

Fynbo, J. U., Möller, P., & Warren, S. J. 1999, Extended LY alpha emission from a damped LY alpha absorber at z=1.93, and the relation between damped LY alpha absorbers and Lyman-break galaxies, MNRAS, 305, 849

Giavalisco, M., Steidel, C. C. & Macchetto, F. D., 1996, Hubble Space Telescope Imaging of Star-forming Galaxies at Redshifts Z¿3, ApJ, 470, 189

Gould, A., & Weinberg, D. H. Imaging the Forest of Lyman Limit Systems, 1996, ApJ, 468, 462

Gray, D. F., 1992, in The Observation and Analysis of Stellar Photospheres 2nd ed., Cambridge Press, New York

Haehnelt, M., Steinmetz, M., & Rauch, M. 1998, Damped Ly alpha Absorber at High Redshift: Large Disks or Galactic Building Blocks?, ApJ, 495, 647

Haehnelt, M., Steinmetz, M., & Rauch, M. 2000, Damped Ly$\alpha$ Absorber and the Faint End of the Galaxy Luminosity Function at High Redshift, ApJ, 534, 594

Harrington, J. P. 1973, The scattering of resonance-line radiation in the limit of large optical depth, MNRAS, 162, 43

Heckman, T. M., Armus, L. & Miley, G. K. 1990, On the nature and implications of starburst-driven galactic superwinds, ApJS, 74, 833

Heiles, C. 1979, HI shells and supershells, ApJ, 229, 533

Heiles, C. 1984, H I shells, supershells, shell-like objects, and 'worms', ApJS, 55, 585

Hu, E. M., McMahon, R. G., & Egami, E. 1996, Detection of a LY alpha Emission-Line Companion to the z=4.69 Quasar BR 1202$-0725, ApJ, 459, L53

Hu, E. M., Cowie L., & McMahon R. G. 1998, The Density of Ly alpha Emitters at Very High Redshift, ApJ, 502, L99

Kamphuis, J., Sancisi R., & van der Hulst T. 1991, An HI superbubble in the spiral galaxy M 101, A&A, 244, L29

Kennicutt, R. C. Jr., Edgar B. K., & Hodge P. W. 1989, Properties of H II region populations in galaxies. II - The HII region luminosity function, ApJ, 337, 761

Koo, B.-C., Heiles C., & Reach W. T. 1991, in The Interstellar Disk-Halo Connection in Galaxies, IAU Symp. 144, ed. H. Bloemen, Kluwer, Dordrecht, p. 165

Koo, B.-C, Heiles C., & Reach W. T. 1992, Galactic worms. I - Catalog of worm candidates, ApJ, 390, 108

Kunth, D., Mas-Hesse, J. M., Terlevich, E., Terlevich, R., Lequeux, J., & Fall, S. M., 1998, HST study of Lyman-alpha emission in star-forming galaxies: the effect of neutral gas flows, A&A, 334, 11

Lee, H. -W., & Ahn S. -H. 1998, Polarization of the Ly alpha from an Anisotrophy Expanding HI Shell in Primeval Galaxies, ApJ, 504, L61

Lee, H. -W., & Blandford, R. 1997, On the polarization of resonantly scattered emission lines - III. Polarization of quasar broad emission lines and broad absorption line troughs, MNRAS, 288, 19

Lehnert, M. D., & Heckman, T. M. 1996, The Nature of Starburst Galaxies, ApJ, 472, 546

Lowenthal, J. D., Koo, D. C., Guzman, R., Gallego, J., Phillips, A. C., Faber, S. M., Vogt, N. P., Illingworth, G. D., & Gronwall, C. 1997, Keck Spectroscopy of Redshift Z approximately 3 Galaxies in the Hubble Deep Field, ApJ, 481, 673

Martin, C. 1998, The Impact of Star Formation on the Interstellar Medium in Dwarf Galaxies. II. The Formation of Galactic Winds, ApJ, 506, 222

Marlowe, A. T., Heckman, T. M., Wyse, R. F. G., & Schommer, R. 1995, Observations of the impact of starbursts on the interstellar medium in dwarf galaxies, ApJ, 438, 563

McKeith C. D., Greve, A., Downes D., & Prada, F. 1995, The outflow in the halo of M 82, A&A, 293, 703

Mihalas, D. 1978, Stellar Atmospheres, W. H. Freeman and Company, San Fransisco

Mo, H. J., Mao, S., & White, S. D. M. 1999, The structure and clustering of Lyman-break galaxies, MNRAS, 304, 175

Möller, P., & Warren, S. J. 1993, Emission from a damped Ly-alpha absorber at Z = 2.81, A&A, 270, 43

Ohyama, Y., Taniguchi, Y., & Terlevich, R. 1997, A New Superwind Wolf-Rayet Galaxy Markarian 1259, ApJ, 480, L9

Osterbrock, D. E. 1962, The Escape of Resonance-Line Radiation from an Optically Thick Nebula, ApJ, 135, 195

Osterbrock, D. E. 1989, Astrophysics of Gaseous Nebulae and Active Galactic Nuclei, University Science Books, California

Petitjean, P., Pecontal, E., Valls-Gabaud, D., & Charlot, S. 1996, A companion to a quasar at redshift Z = 4.7, Nature, 380, 411

Pettini, M., Shapley, A. E., Steidel, C. C., Cuby, J. -G., Dickinson, M., Moorwood, A. F. M., Adelberger, K. L., & Giavalisco, M. 2001, The Rest-Frame Optical Spectra of Lyman Break Galaxies: Star Formation, Extinction, Abundances, and Kinematics, ApJ, 554, 981

Press, W. H., Flannery, B. P., Teukolsky, S. A., & Vetterling, W. T. 1989, Numerical Recipes, Cambridge Press, New York

Prochaska, J. X., & Wolfe, A. M. 1997, The Kinematics of the Damped Lyman Alpha Protogalaxies, AAS, 190, #47.04

Reach, W. T., Heiles, C., & Koo, B.-C. 1993, in AIP Conf. Proc. 278, Back to Galaxy, ed. S. S. Holt and F. Verter (New York, AIP), p.67.

Rybicki, G. B., & Hummer, D. G. 1978, A generalization of the Sobolev method for flows with nonlocal radiative coupling, ApJ, 219, 654

Rybicki, G. B., & Lightman, A. P. 1979, Radiative Processes in Astrophysics, John Wiley & Sons, New York

Sengupta, S. 1994, Resonance-Line Polarization in Expanding Spherical Atmospheres - Solution in the Comoving Frame, MNRAS, 269, 265

Silich, S., & Tenorio-Tagle, G. 1998, On the fate of processed matter in dwarf galaxies, MNRAS, 299, 249

Sobolev, V. 1960, Moving Envelopes of Stars, Harvard Univ. Press, Cambridge, Mass.

Spitzer, L. 1978, Physical Processes in the Interstellar Medium, John Wiley & Sons, New York

Steidel, C. C., Adelberger, K. L., Dickinson, M., Giavalisco, M., Pettini, M., & Kellogg, M. 1998, ApJ, 492, 428

Steidel, C. C., Giavalisco, M., Dickinson, M., & Adelberger, K. L. 1996, Spectroscopy of Lyman Break Galaxies in the Hubble Deep Field, AJ, 112, 352

Steidel, C. C., Giavalisco, M., Pettini, M., Dickinson, M., & Adelberger, K. L. 1996, Spectroscopic Confirmation of a Population of Normal Star-forming Galaxies at Redshifts Z¿3, ApJ, 462, L17

Suchkov, A. A., Balsara, D. S., Heckman, T. M., Leitherner, C., 1994, Dynamics and X-ray emission of a galactic superwind interacting with disk and halo gas, ApJ, 430, 511

Tenorio-Tagle, G., Silich, S. A., Kunth, D., Terlevich, E., & Terlevich, R. 1999, The evolution of superbubbles and the detection of Ly$\alpha$ in star-forming galaxies, MNRAS, 309, 332

Terlevich R., & Melnick J. 1981, The dynamics and chemical composition of giant extragalactic HII regions, MNRAS, 195, 839

Trager S. C., Faber S. M., Dressler A., & Oemler A. 1997, Galaxies at Z$\approx$4 and the Formation of Population II, ApJ, 485, 92

Warren S. J., & Möller P. 1996, Spectroscopy of emission from a damped Ly$\alpha$ absorber at z=2.81, A&A, 311, 25

## Appendix
## A. SCATTERING OPTICAL DEPTH

In this subsection we give a brief model description and a basic atomic physics for the Monte Carlo code, which computes the profile of the emergent Ly$\alpha$ photons scattered inside an optically thick and expanding medium.

The scattering cross section in the rest frame of the scatterer is given by

$$\begin{aligned} \sigma_\nu &= \sigma(x) = \frac{\pi e^2}{m_e c} f_{osc} \frac{\Gamma/4\pi^2}{(\nu-\nu_0)^2 + (\Gamma/4\pi)^2} \\ &= \frac{\pi e^2}{m_e c} f_{osc} \frac{1}{\pi \Delta\nu_D} \frac{a}{x^2+a^2}, \end{aligned} \tag{A1}$$

where $f_{osc}$ is the oscillator strength, $m_e$ is the electron mass (Rybicki & Lightman 1979).

The scattering optical depth $\tau_{12}(x)$ of a line photon with frequency shift $x$ and wave vector $\mathbf{k_i}$ corresponding to the distance from the position $\mathbf{r_1}$ to $\mathbf{r_2}$ is computed to determine the subsequent scattering position in the Monte Carlo calculation. Due to the Hubble-type velocity field and a constant density field inside the scattering medium, we get the same Hubble-type flow if we make a translation so that $\mathbf{r_1}$ coincides with the new origin. The line center frequency $\nu_0'(r)$ in the

observer's frame differs from that in the scatterer's rest frame by the Doppler shift, which is given by

$$\nu_0'(r) = \nu_0(1 - H_v r/c + v_{loc}/c), \qquad \text{(A2)}$$

where $r$ is the distance from the new origin $\mathbf{r_1}$ and $v_{loc}$ is the local velocity of the scatterer due to the thermal motion.

The normalized frequency shift $x'(r)$ is now simply given by

$$x'(r) = x - s + u, \qquad \text{(A3)}$$

where $u \equiv v_{loc}/v_{th}$. Therefore the scattering cross section $\sigma(x)$ becomes a function of the position due to the coupling of the line center frequency and the position determined by the expansion of the medium.

The scatterers are assumed to be governed by a Maxwellian distribution, that is,

$$n = n_0 \int dv_{loc}\ f(v_{loc}), \qquad \text{(A4)}$$

where

$$\begin{aligned} f(v_{loc}) &= (\pi v_{th})^{-1/2} \exp\left[-(v_{loc}/v_{th})^2\right] \\ &= (\pi v_{th})^{-1/2} e^{-u^2} \end{aligned} \qquad \text{(A5)}$$

is the Maxwellian distribution function.

Combining Eqs. (A.1-A.5), we obtain

$$\begin{aligned} \tau_{12}(s) &= \int_{-\infty}^{\infty} du \int_0^s ds'\ n_0\ f(u)\sigma[x'(s')] \\ &= \tau_0 \int_{-\infty}^{\infty} du\ e^{-u^2} \left[\tan^{-1}\left(\frac{u+x}{a}\right)\right. \\ &- \left.\tan^{-1}\left(\frac{u+x-s}{a}\right)\right]. \end{aligned} \qquad \text{(A6)}$$

Here, $\tau_0$ is the Sobolev-type optical depth defined by Eq.(10).

## B. MONTE CARLO APPROACH

In this subsection, we present a detailed description of the Monte Carlo procedure. There are a few approaches to the resonance line transfer in an optically thick and static medium (Osterbrock 1962, Adams 1972, Harrington 1973, Sengupta 1994, Gould & Weinberg 1996). However, there are also studies on the line formation in a thick expanding medium (e.g. Rybicki & Hummer 1978).

The Sobolev approximation has been one of the most favored methods in dealing with the line transfer in an expanding medium. However, the validity of the Sobolev method is limited to the cases where the bulk flow is much larger than the thermal velocity and the optical depth of the medium does not greatly exceed unit. This is because the scattering in the damping wing is no more negligible in an optically thick medium where the typical line center optical depth $\tau_c \gtrsim 10^4$. Therefore we develop a Monte Carlo code in which the scattering in the damping wing is carefully considered in a thick moving medium.

The Monte Carlo code begins with the choice of the frequency and the propagation direction $\mathbf{k_i}$ of the incident photon from an assumed Ly$\alpha$ profile.

Then we determine the next scattering site separated from the initial point by the normalized propagation length $s$ defined by Eq.(6), which corresponds to the optical depth of $\tau = -\ln(\mathbf{R})$, where $\mathbf{R}$ is a uniform random number in the interval $(0, 1)$. Due to the unwieldiness of the inverse relation of Eq.(9), we tabulate the normalized path length $s(x, \tau)$ in advance and look up the table to find $s$ by the linear interpolation. For our numerical computation, the range of $x$ is taken to be from $-4s_{max}$ to $4s_{max}$ with a step of $\Delta x = 0.5$, and $\tau$ runs from 0 to $4s_{max}$ with a step of 0.002, where $s_{max} = 10$ is assumed.

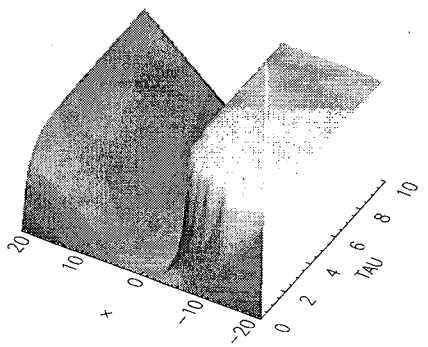


**Fig. B1.**— A surface plot of the $s(x, \tau)$ table. $x \equiv \Delta\nu/\Delta\nu_D$ and $TAU = \tau$ represents the optical depth. The plateau on the right top side corresponds to $s = 2s_{max} + 1$.

In Fig. B1 we present the $s(x, \tau)$ table as a surface plot. We restrict the propagating length $s$ to be $0 < s < 2s_{max}$, and set $s = 2s_{max} + 1$ if the true value of $s(x, \tau)$ exceeds $2s_{max}$. A U-shaped distribution of $s$ is seen in the figure, which is naturally explained by the fact that the scattering medium is transparent for extreme blue and red photons.

The emitted photon traverses a distance $s$ found by the above procedure and is scattered if $s < 2s_{max}$. In this scattering event the frequencies of the absorbed photon and the re-emitted one in the rest frame of the scatterer should be matched. For the case of an optically thin and expanding medium, this frequency matching is combined with the Sobolev approximation to yield the absorption profile in the form of the Dirac delta function.

As mentioned earlier, in contrast with the case of a thin medium, for a very thick medium the scattering in the damping wing is not negligible. A good care need to be exercised to distinguish the scattering in the damping wing from the resonance scattering, because they show quite different behaviors in the properties including the scattering phase function and the polarization (Lee & Blandford 1997).

Because the natural line width is much smaller than the Doppler width, scatterers that can resonantly scatter the incident photon has a sinlge value for the local velocity component along the propagation direction. However, when the scattering occurs in the damping wing, the local velocity of the scatterer may run a rather large range. Therefore, in order to enhance the efficiency of the Monte Carlo method, it is desirable to determine the scattering type before we determine the local velocity $\mathbf{u}$ of the scatterer.

We present a more quantitative argument about the preceding remarks. Under the condition that a given photon is scattered by an atom located at a position $s$, the local velocity component $u$ along the direction $\mathbf{k_i}$ is simply given by

$$f(u) \propto \frac{\exp(-u^2)}{(u-b)^2+a^2}, \tag{B1}$$

where $b = s - x$. The normalization condition is used to get

$$f(u) = \frac{\exp(-u^2)}{(u-b)^2+a^2}\left[\frac{\pi}{a}H(a,b)\right]^{-1}. \tag{B2}$$

Here, the Voigt function $H(a,b)$ is evaluated by a series expansion in $a$, i.e.,

$$H(a,b) = H_0(a,b) + aH_1(a,b) + a^2H_2(a,b) + \cdots, \tag{B3}$$

where $H_n(a,b)$, $n = 0, 1, 2, 3$ are tabulated by Gray (1992).

Because of the smallness of $a$, the function $f$ has a sharp peak around $u \approx b$, for which the scattering may be regarded as purely resonant. Therefore, the probability $P_r$ that a given scattering is resonant is approximately given by

$$P_r \simeq \int_{-\infty}^{\infty} d(\Delta u)\frac{e^{-b^2}}{(\Delta u)^2+a^2}\left[\frac{\pi}{a}H(a,b)\right]^{-1} = \frac{e^{-b^2}}{H(a,b)}. \tag{B4}$$

The probability that a scattering occurs in the damping wing is

$$P_{nr} = 1 - P_r. \tag{B5}$$

In the code we determine the scattering type in accordance with the scattering type probabilities $P_r$ and $P_{nr}$. If a scattering is chosen to be non-resonant, then the scattering occurs in the damping wing, and $u$ is chosen according to the velocity probability distribution given by Eq.(B2). Otherwise the scattering is chosen to be resonant, and we set $u = b$. Furthermore, the Ly$\alpha$ transition is the doublet with the two excited states $j_{3/2,1/2}$ having the energy difference of only $\Delta V = 1.34$ km s$^{-1}$ in terms of velocity units, where the transition with the upper $j_{3/2}$-state has twice larger oscillator strength than the other. This fine point is not important in the computation of the profile and is ignored in the current work. However, if the polarization is concerned, this point should be also considered, because each resonant transition has a different scattering phase function that depends on the angular momentum quantum numbers of the ground and excited states. One example of this consideration can be found in Lee & Ahn (1998).

We give the propagation direction $\mathbf{k_f}$ of a scattered photon in accordance with the isotropic phase function. The scattered velocity component $v_\perp$ perpendicular to the initial direction $\mathbf{k_i}$ on the plane spanned by $\mathbf{k_i}$ and $\mathbf{k_f}$ is also governed by a Maxwell-Boltzman velocity distribution, which is numerically obtained using the subroutine *gasdev* suggested by Press et al. (1989). The contribution $\Delta x$ of the perpendicular velocity component $v_\perp$ to the frequency shift along the direction of $\mathbf{k_f}$ is obviously

$$\Delta x = v_\perp[1 - (\mathbf{k_i}\cdot\mathbf{k_f})^2]^{1/2}/c. \tag{B6}$$

Therefore, the frequency shift $x_f$ of the scattered photon is given by

$$x_f = x_i - u + u(\mathbf{k_i}\cdot\mathbf{k_f}) + v_\perp[1 - (\mathbf{k_i}\cdot\mathbf{k_f})^2]^{1/2}, \tag{B7}$$

where $x_i$ is the frequency shift of the incident photon.

In each scattering event the position of the scattered photon is checked and if it is out of the medium we collect this photon according to its frequency and escaping direction. The whole procedure is repeated to collect typically about $10^3$ photons in each frequency bin.